

Functional MRI Safety and Artifacts during Deep Brain Stimulation: Experience in 102 Patients

Alexandre Boutet, MD, MSc* • Tanweer Rashid, PhD* • Ileana Hancu, PhD • Gavin J. B. Elias, BA • Robert M. Gramer, BSc • Jürgen Germann, MSc • Marisa Dimarzio, BS • Bryan Li, MRT • Vijayashankar Paramanandam, MBBS • Sreeram Prasad, MBBS • Manish Ranjan, MCh • Ailish Coblentz, MBBS • Dave Gwun • Clement T. Chow, BKin • Ricardo Maciel, MD, MSc • Derrick Sob, MD • Eric Fiveland, MS • Mojgan Hodaie, MD, MSc • Suneil K. Kalia, MD, PhD • Alfonso Fasano, MD, PhD • Walter Kucharczyk, MD • Julie Pilitsis, MD, PhD • Andres M. Lozano, MD, PhD


From the Joint Department of Medical Imaging, University of Toronto, Toronto, Canada (A.B., A.C., W.K.); Division of Neurosurgery, Toronto Western Hospital, University Health Network, 399 Bathurst St, WW 4-437, Toronto, ON, Canada M5T 2S8 (A.B., G.J.B.E., R.M.G., J.G., B.L., V.P., S.P., M.R., A.C., D.G., C.T.C., R.M., D.S., M.H., S.K.K., A.F., W.K., A.M.L.); Department of Neuroscience and Experimental Therapeutics, Albany Medical College, Albany, NY (T.R., M.D., J.P.); Edmond J. Safra Program in Parkinson's Disease, Morton and Gloria Shulman Movement Disorders Clinic, Toronto Western Hospital, UHN, Division of Neurology, University of Toronto, Toronto, Ontario, Canada (I.H., V.P., S.P., R.M., D.S., A.F.); GE Global Research Center, Niskayuna, NY (E.F.); Krembil Brain Institute, Toronto, Canada (A.F.); and Department of Neurosurgery, Albany Medical Center, Albany, NY (J.P.). Received March 10, 2019; revision requested May 17; revision received June 10; accepted June 21. Address correspondence to A.M.L. (e-mail: lozano@uhnresearch.ca).

Supported in part by GE Global Research, the RR Tasker Chair in Functional Neurosurgery at University Health Network, and the Tier 1 Canada Research Chair in Neuroscience. M.R. supported by a Weston Brain Institute grant/advisor fellowship.

*A.B. and T.R. contributed equally to this work.

Conflicts of interest are listed at the end of this article.

See also the editorial by Martin in this issue.

Radiology 2019; 293:174–183 • <https://doi.org/10.1148/radiol.2019190546> • Content codes: 

Background: With growing numbers of patients receiving deep brain stimulation (DBS), radiologists are encountering these neuro-modulation devices at an increasing rate. Current MRI safety guidelines, however, limit MRI access in these patients.

Purpose: To describe an MRI (1.5 T and 3 T) experience and safety profile in a large cohort of participants with active DBS systems and characterize the hardware-related artifacts on images from functional MRI.

Materials and Methods: In this prospective study, study participants receiving active DBS underwent 1.5- or 3-T MRI (T1-weighted imaging and gradient-recalled echo [GRE]–echo-planar imaging [EPI]) between June 2017 and October 2018. Short- and long-term adverse events were tracked. The authors quantified DBS hardware-related artifacts on images from GRE-EPI (functional MRI) at the cranial coil wire and electrode contacts. Segmented artifacts were then transformed into standard space to define the brain areas affected by signal loss. Two-sample *t* tests were used to assess the difference in artifact size between 1.5- and 3-T MRI.

Results: A total of 102 participants (mean age \pm standard deviation, 60 years \pm 11; 65 men) were evaluated. No MRI-related short- and long-term adverse events or acute changes were observed. DBS artifacts were most prominent near the electrode contacts and over the frontoparietal cortical area where the redundancy of the extension wire is placed subcutaneously. The mean electrode contact artifact diameter was 9.3 mm \pm 1.6, and 1.9% \pm 0.8 of the brain was obscured by the coil artifact. The coil artifacts were larger at 3 T than at 1.5 T, obscuring 2.1% \pm 0.7 and 1.4% \pm 0.7 of intracranial volume, respectively ($P < .001$). The superficial frontoparietal cortex and deep structures neighboring the electrode contacts were most commonly obscured.

Conclusion: With a priori local safety testing, patients receiving deep brain stimulation may safely undergo 1.5- and 3-T MRI. Deep brain stimulation hardware-related artifacts only affect a small proportion of the brain.

© RSNA, 2019

Online supplemental material is available for this article.

Multiple neurologic disorders are thought to arise from dysfunctional neuronal circuits. Modulation of malfunctioning circuits can be achieved with therapies such as deep brain stimulation (DBS) (1). In DBS, electrical stimulation is delivered through implanted brain electrodes (2,3). DBS is best established as a therapeutic tool for movement disorders such as Parkinson disease, essential tremor, and dystonia (1,3). DBS is also being investigated as a treatment for psychiatric (4) and cognitive disorders (3). To date, more than 150 000 individuals have been implanted with DBS worldwide (5). Due to safety concerns, the ability to undergo MRI following DBS implantation

is highly restricted. Because patients receiving DBS may require a wide range of MRI sequences for clinical purposes, and because MRI has been shown to be a valuable research tool in this population, additional data expounding the safety profile of MRI in individuals receiving DBS would be beneficial.

Owing to safety concerns, MRI guidelines for scanning individuals receiving DBS are restrictive, largely limiting diagnostic uses. Strict safety guidelines (6–8) have been implemented after MRI-related adverse events (9): two cases of implantable pulse generator (IPG) failure during 1.5-T brain MRI; one case of temporary peri-electrode edema

Abbreviations

DBS = deep brain stimulation, EPI = echo-planar imaging, GRE = gradient-recalled echo, IPG = implantable pulse generator, SAR = specific absorption rate

Summary

With a priori local safety testing, 1.5- and 3-T MRI may be safely performed in participants with implanted deep brain stimulation (DBS) systems as the DBS artifact only affects a small proportion of the brain.

Key Results

- The mean electrode contact artifact diameter was 9.3 mm, and 1.9% of the brain was obscured by the coil artifact.
- Although the coil artifact caused by deep brain stimulation neuromodulation systems is larger at higher magnetic field strength (2.1% of intracranial volume at 3 T vs 1.4% at 1.5 T [$P < .001$]), it remains mostly limited to the superficial frontoparietal cortex and structures neighboring the electrode contacts; thus, most of the brain is visible and fit for analyses such as functional MRI.

during 1.5-T brain MRI thought to be related to unwanted tension on the externalized DBS leads during scanning; one case of peri-electrode hemorrhage during 1.0-T lumbar spine MRI thought to be due to the atypical placement of bilateral IPGs, one of which was abdominal (10); and one case of transient dystonic movements during 1.0-T brain MRI thought to be due to an occult peri-electrode injury (11). At present, MRI-conditional DBS neuromodulation systems from Medtronic (Minneapolis, Minn) (7), Boston Scientific (Marlborough, Mass) (6), and Abbott (Chicago, Ill) (8) have been approved by the U.S. Food and Drug Administration for MRI at specific magnetic field strengths (ie, 1.5 T) and with specific heating-related thresholds (eg, specific absorption rate [SAR]). However, there is considerable interest in investigating the safety of MRI at higher magnetic fields (eg, 3 T, 7 T) and of the less commonly used experimental sequences given their potential as future clinical tools (12,13).

To date, investigators have used phantom models replicating the configuration of DBS neuromodulation devices in individuals to explore the MRI safety of DBS hardware outside of vendor guidelines (14–19). The main safety issue addressed with phantom experiments is heating of the DBS neuromodulation system (20). Higher heating is expected with higher magnetic field strengths and the use of body transmit coils, which optimizes signal-to-noise ratio and speed of acquisition while minimizing distortion of images obtained with MRI distortion (17). Experiments in phantoms have yielded inconsistent results with regard to safe MRI of DBS; this is due in part to the heterogeneous and continually evolving DBS and MRI hardware (21,22). Notably, recent phantom studies have demonstrated an acceptable temperature rise at the electrodes when using 3-T MRI and a body transmit coil (15,19,23).

Neuroimaging has furthered our understanding of the mechanisms underlying the effects of DBS. In particular, functional MRI has shown engagement of motor and emotional circuits during DBS stimulation for Parkinson disease (23,24) and obsessive-compulsive disorder (25), respectively. However, the metallic susceptibility artifact associated with the DBS device limits the assessment of certain areas (15).

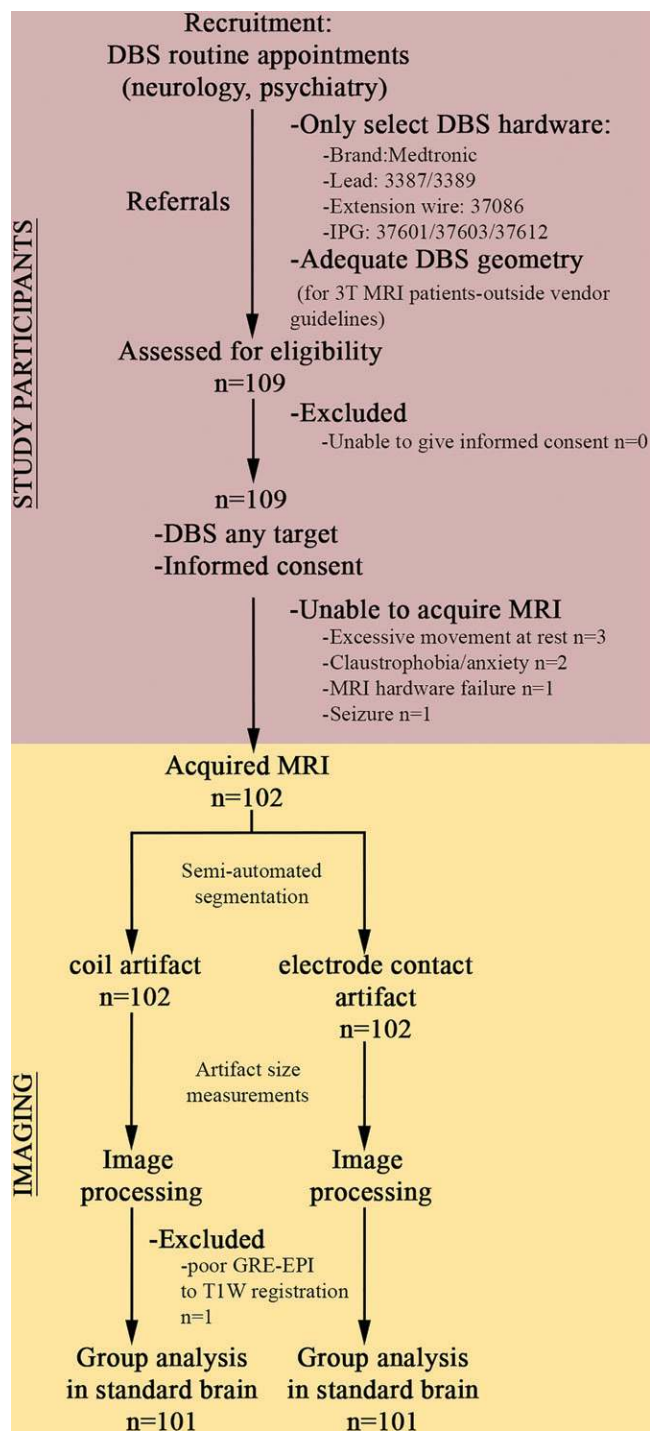


Figure 1: Study flowchart shows recruitment of study participants with referrals from primary responsible physicians and inclusion and exclusion criteria. Steps for image analysis are also shown. DBS = deep brain stimulation, GRE-EPI = gradient-recalled echo–echo-planar imaging, T1 W = T1-weighted.

We hypothesized that, under specific conditions, participants with DBS could safely undergo 1.5- and 3-T MRI and that the associated artifacts at functional MRI would be limited and not prohibit analysis. Following published safety data (15,19,23), we aimed to (a) share our experience performing MRI in a large number of study participants receiving DBS both within and

outside of vendor guidelines and (b) characterize the artifacts on images from functional MRI.

Materials and Methods

In a previous study (15), we reported on 41 participants included in our current study. The current study expands on that study by using body transmit-receive coils and includes analyses characterizing DBS metallic artifacts seen on images from functional MRI.

Following ethical approval (institution 1 [Toronto Western Hospital, Toronto, Ontario, Canada], #14-8255; institution 2 [Albany Medical College, Albany, NY], #4683/5082), participants included in this prospective study (clinicaltrials.gov identifier: NCT03153670) provided written informed consent. Study protocols and data generated during the study are available from the corresponding author by request. The study was supported by GE Global Research, the RR Tasker Chair in Functional Neurosurgery at University Health Network, and a Tier 1 Canada Research Chair in Neuroscience. The supporting party (GE Global Research) contributed to the data acquisition and analysis (I.H., E.F.). The corresponding author confirms that he had control of all data and information throughout the study.

Study Participants

We recruited participants at the DBS clinics (Fig 1). Participants were included if they (a) were receiving active DBS at any therapeutic targets, (b) could provide written informed consent, and (c) had specific models of Medtronic DBS hardware, including DBS leads (model 3387 or 3389, 28 cm; Medtronic), extension wire (model 37086, 60 cm; Medtronic), and IPG (Activa PC 37601, Activa RC 37612, or Activa SC 37603; Medtronic). The DBS models used are summarized in Figure 2. Participants undergoing 3-T MRI were also required to have DBS hardware geometry similar to previous phantoms (15,19,23), with redundant extension wire coiled into an extension loop (approximately 2 cm in diameter) under the scalp and the remainder of excess wire coiled behind a subclavicular IPG (Fig 3). Participants were excluded if they were unable to provide informed consent (eg, they had cognitive, psychologic, or communication impairments). MRI could not be performed in participants with excessive movement at rest (usually when DBS was turned off) or in participants who were too anxious or claustrophobic at the time of the MRI.

From June 2017 to October 2018, we performed MRI at two academic medical institutions in 102 participants receiving DBS with fully internalized electrodes (Table 1). We used T1-weighted three-dimensional spoiled gradient-recalled echo (GRE)-echo-planar imaging (EPI) sequences; MRI hardware

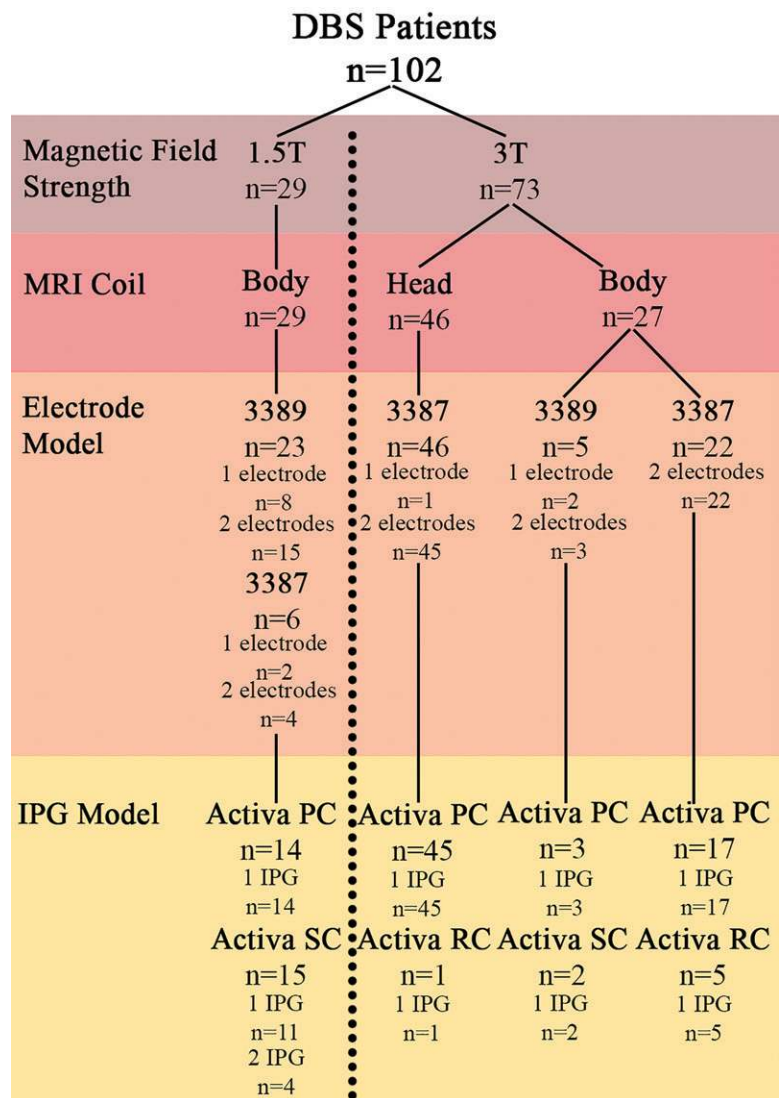


Figure 2: Summary of models used for MRI and deep brain stimulation (DBS). Hardware was obtained from Medtronic (Minneapolis, Minn). Participants were scanned at 1.5 T or 3 T with a multi-array transmit-receive coil (body) or a quadrature transmit-receive head coil (head). Electrode models 3387 or 3389 and Activa PC, Activa RC, or Activa SC implantable pulse generators (IPGs) were used. Participants had unilateral or bilateral electrodes and a single IPG or dual IPGs.

and pulse sequences are described in detail in Tables 2 and 3, respectively.

Of the 102 participants, 29 underwent 1.5-T MRI and 73 underwent 3-T MRI. The 1.5-T MRI examinations were performed according to Medtronic guidelines and with use of bipolar stimulation (7). The 3-T MRI examinations were performed with DBS turned on at native DBS settings (eg, monopolar). This is in contrast to vendor recommendations that prohibit the use of field strengths other than 1.5 T and turning on the DBS at current settings other than bipolar during MRI (7). The importance of using native stimulation settings when acquiring experimental data was previously demonstrated (23).

We assessed short-term adverse effects with complete neurologic examination immediately after MRI (institution

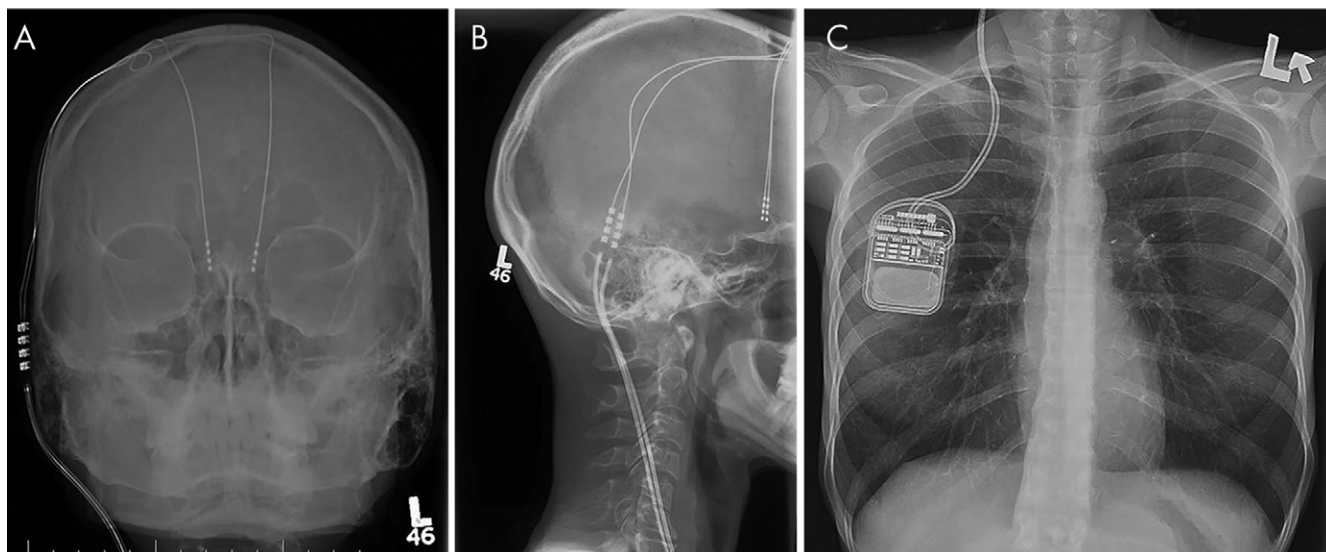


Figure 3: Radiographs of deep brain stimulation (DBS) device. Typical DBS hardware configurations used at our institution are seen on radiographs of, *A*, skull, *B*, neck, and, *C*, chest. Cranial loops of coiled extension wire have a diameter of approximately 2 cm. The remaining excess extension wire is coiled behind the thoracic implantable pulse generator.

1 and 2) and 1 week after MRI neurosurgical follow-up (institution 2). Neurologic examinations were performed by a fellowship-trained neurosurgeon with 8 years of experience (M.R.), a fellowship-trained neurologist with 8 years of experience, and a registered nurse with 7 years of experience. The examination consisted of evaluations of motor, sensory (upper and lower limbs), and cranial nerve functions as well as assessment of alertness and orientation. Any clinical change from baseline was considered an adverse event. Short-term adverse effects were also assessed with review of the MRI and DBS impedance changes. Signal intensity changes adjacent to the neurostimulator, other than the typical metallic artifact, were taken as an adverse event. We interpreted low or intermediate signal intensity on T1-weighted images as edema. Low signal intensity on GRE-EPI images was interpreted as hemorrhage (A.B., a radiology trainee with 3 years of experience, and W.K., a neuroradiologist with 30 years of experience). We also recorded therapy DBS system impedances before and after MRI using an Activa Patient Programmer (model 37642; Medtronic) to ensure the electrical circuit integrity of the system and the stability of peri-electrode tissue (eg, absence of gross edema or hemorrhage). Only gross impedance changes would be meaningful given that (*a*) very low (bipolar current <250 Ω) or very large (monopolar current >2000 Ω) impedance values are meaningful in conjunction

Table 1: Summary of Primary DBS Indications and DBS Targets

Parameter	Value
Mean age (y)*	60.0 \pm 11.4 (26–80)
Women	55.6 \pm 14.3 (26–80)
Men	62.5 \pm 8.5 (28–78)
Sex	
Women	37 (36)
Men	65 (64)
Primary DBS indication and target	
Parkinson disease/subthalamic nucleus	69 (68)
Parkinson disease/globus pallidus interna	16 (15)
Dystonia/globus pallidus interna	1 (1)
Major depressive disorder/subcallosal cingulate cortex	4 (4)
Anorexia nervosa/subcallosal cingulate cortex	8 (8)
Alzheimer disease/fornix	3 (3)
Epilepsy/anterior thalamic nucleus	1 (1)

Note.—Unless otherwise specified, data are numbers of participants ($n = 102$), with percentages in parentheses. DBS = deep brain stimulation.

* Data are means \pm standard deviations, with ranges in parentheses.

with a change in clinical efficacy, (*b*) acute impedance changes can be seen with stimulation (26), and (*c*) slight impedance variations may be routinely seen (27). Finally, long-term adverse effects were assessed at the latest routine DBS visits at least 1 month after MRI; any clinical change from baseline was considered an adverse event.

We also measured parameters correlated with implant heating. SAR values were extracted from the Digital Imaging Communications in Medicine headers. The root mean square value of the MRI effective component of the radiofrequency magnetic field (B_1), or B_{1+rms} , was computed retroactively by uploading on an MRI software (revision version 26.0; GE Healthcare, Chicago, Ill) protocols scanned on a selected number of participants.

Table 2: MRI Hardware Used at Both Institutions

Institution	MRI Machines	Coils	No. of Participants
1	3.0-T Signa MRI scanner with HDx version 16.0_V02_1131.a software	3.0-T HD multiarray body transmit-receive coil (eight channels, model 2380637-2)	22
		Quadrature transmit-receive head coil (model 2376114)	46
2	1.5-T Signa MRI scanner with HDxT version 23.0_V02_1406.a software	1.5-T HD eight-channel body transmit brain array receive coil	29
	3.0-T Signa MRI scanner with Signa Architect version 27\LX\ MR software (software release: DV26.0_R01_1725.a)	Multi-array body transmit-receive coil (24 channels, HNU coil)	5

Note.—All equipment was manufactured by GE Healthcare.

Table 3: Pulse Sequences and Associated Parameters Used for Scanning Participants Receiving DBS

Parameter	1.5 T: Institution 2		3 T: Institution 1				3 T: Institution 2	
	GRE-EPI Multiphase fMRI with Body Transmit Coil	T1-weighted 3D SPGR MRI with Body Transmit Coil	GRE-EPI Multiphase fMRI with Body Transmit Coil	T1-weighted 3D SPGR MRI with Body Transmit Coil	GRE-EPI Multiphase fMRI with Head Transmit-Receive Coil	T1-weighted 3D SPGR MRI with Head Transmit-Receive Coil	GRE-EPI Multiphase fMRI with Body Transmit Coil	T1-weighted 3D SPGR MRI with Body Transmit Coil
TR (msec)	3011	12.88	2151	8	3010	8	3011	7.58
TE (msec)	40	5.48	30	3	30	3	35	3.196
TI (msec)	NA	0	NA	450	NA	450	NA	0
BW (kHz)	250	16	62.5	31.25	62.5	31.25	250	31.25
FOV (mm)	200 × 200	200 × 180	240 × 240	256 × 256	240 × 240	256 × 256	220 × 220	220 × 200
FA (degrees)	90	12	86	20	84	20	85	12
Section thickness (mm)	3.0	1.8	4.0	1	3.0	1	4.5	0.8
Gap (mm)	0	0	0	0	0	0	0	0
ETL	1	1	1	1	1	1	1	1
Matrix	64 × 64	512 × 512	64 × 64	256 × 256	64 × 64	256 × 256	64 × 64	512 × 512
Frequency (direction)	L/R	A/P	L/R	A/P	L/R	A/P	L/R	A/P
No. of signals acquired	1	1	1	1	1	1	1	1

Note.—A/P = anterior-posterior, BW = bandwidth, DBS = deep brain stimulation, ETL = echo train length, FA = flip angle, fMRI = functional MRI, FOV = field of view, GRE-EPI = gradient-recalled echo-echo-planar imaging, L/R = left-right, NA = not applicable, SPGR = spoiled gradient-recalled, TE = echo time, TI = inversion time, TR = repetition time, 3D = three-dimensional.

In other words, B_{1+rms} is a measure of the average effective magnetic field generated by the radiofrequency transmit coil.

Neuroimaging Analyses

We characterized DBS neurostimulator artifacts (coil and electrode contact artifacts) on images from GRE-EPI MRI by using a semiautomated segmentation method (Figs E1, E2 [online]). We also performed group analysis of commonly obscured brain structures. Finally, to demonstrate feasibility of resting-state networks analysis in participants receiving DBS, we performed a limited resting-state networks analysis. Detailed methods are given in Figure 4 and Appendix E1 (online).

Statistical Analysis

Two-sample *t* tests (unequal variance) were used to assess the difference in artifact size and SAR between 1.5- and 3-T MRI. *P* < .05 was considered indicative of a statistically significant difference. Statistics were done by using R-Project software (version 3.4.3, <https://www.r-project.org/>, open source).

Results

Demographics of Study Cohort

Our study cohort consisted of 102 participants with a mean age (\pm standard deviation) of 60 years \pm 11; 65 participants

were men and 37 were women. One patient was excluded from the neuroimaging analyses.

Adverse Events

There were no MRI-related adverse events in the 102 participants receiving DBS who underwent MRI at our institutions at both 1.5 T ($n = 29$) and 3 T ($n = 73$). Specifically, no acute or long-term adverse effects were detected. The mean time between MRI and the latest DBS clinic visit was 488 days \pm 209 ($n = 97$, five patients without DBS clinic visit at the time of publication). MRI demonstrated no acute brain changes. The mean DBS system impedance before MRI was 1023 Ω (range, 548–1693 Ω) on the right and 1136 Ω (range, 605–2946 Ω) on the left. After MRI, the mean DBS system impedance was 1034 Ω (range, 717–1943 Ω) on the right and 1106 Ω (range, 584–2863 Ω) on the left.

SAR and B_{1+rms}

We compared the SAR with body transmit coils at both field strengths (Table 4). SAR values were lower at 1.5 T than at 3 T for both GRE-EPI (functional MRI) and T1-weighted MRI ($P < .001$). SAR values at both GRE-EPI (mean SAR: 0.031 W/Kg \pm 0.002) and T1-weighted MRI (mean SAR: 0.078 W/Kg \pm 0.006) were within the vendor guidelines at 1.5 T (≤ 0.1 W/Kg). At 3 T, SAR values were 0.221 W/Kg \pm 0.054 and 0.397 W/Kg \pm 0.046 for GRE-EPI and T1-weighted MRI, respectively. Mean SAR values with the 3-T quadrature transmit-receive head coil were 0.41 W/Kg \pm 0.14 (range, 0.24–1.09 W/Kg) and 0.51 W/Kg \pm 0.07 (range, 0.21–0.63 W/Kg) for T1-weighted three-dimensional spoiled GRE imaging and GRE-EPI, respectively. For GRE-EPI, B_{1+rms} values were 0.77 μ T at 1.5 T and 0.60–0.69 μ T at 3 T. For T1-weighted three-dimensional spoiled GRE imaging, B_{1+rms} values were 1.13 μ T at 1.5 T and 1.16–1.40 μ T at 3 T (Table E1 [online]). Approximately 10% variability in the B_{1+rms} values was noted in each of the four hardware configurations, depending on the number of sections prescribed to accommodate each participant's anatomy.

Functional MRI Artifact Associated with DBS Hardware

Metallic susceptibility artifacts were most prominent in two areas: circumferentially along the DBS lead (particularly around the electrode contacts) and in the parietal area subjacent to the subgaleal wire coil (Fig 5). The contact artifact diameters and the actual and proportional (relative to intracranial volume) coil artifact volumes were measured for the whole cohort and for the 1.5-T and 3-T cohorts separately (Table 5). For the whole cohort, the mean contact artifact diameter was 9.3 mm \pm 1.6; 1.9% \pm 0.8 of the intracranial volume was obscured by the coil artifact. The largest coil artifacts were seen in the four participants with bilateral IPG obscuring 1.98%–1.99% of the gray matter. The coil artifacts were smaller at 1.5 T (1.4% \pm 0.7 of intracranial volume) than at 3 T (2.1% \pm 0.7 of intracranial volume) ($P < .001$), whereas no difference was seen for the contact artifact diameters ($P = .1$).

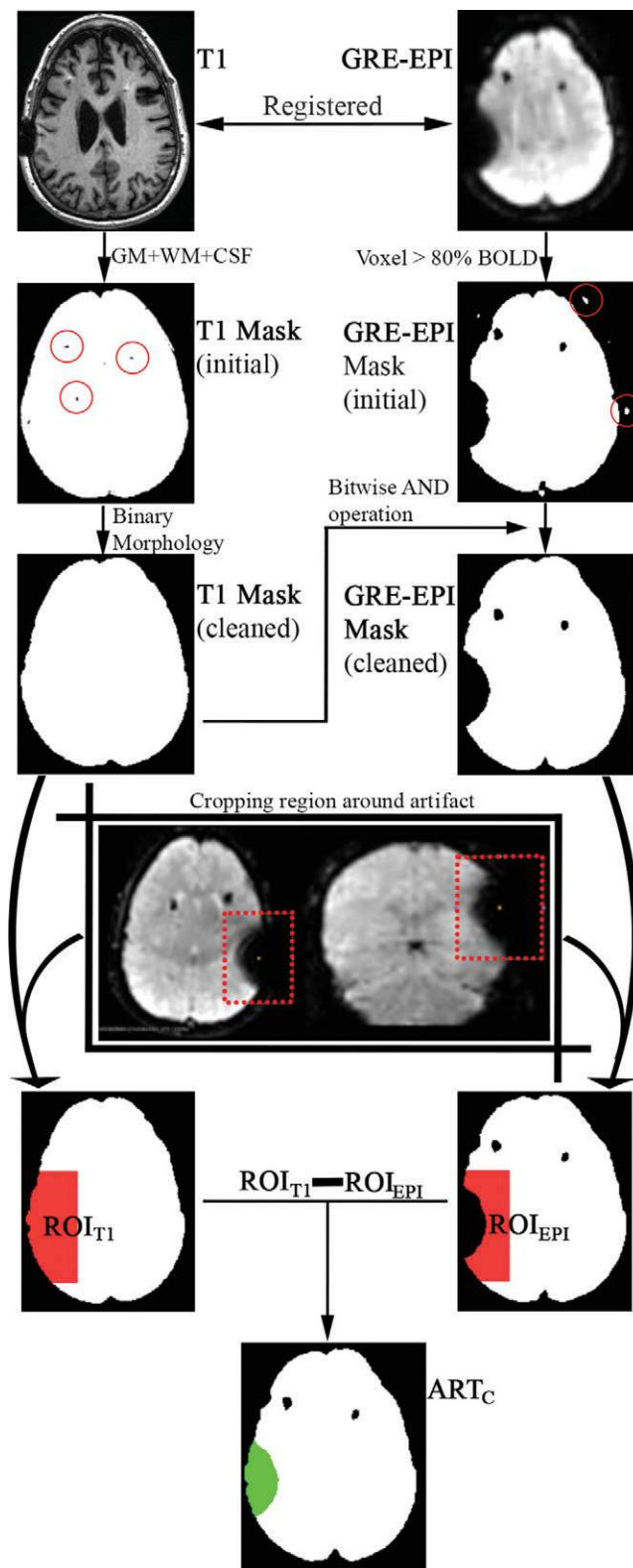


Figure 4: Methods used for semiautomatic frontoparietal artifact segmentation. Similar methods were used to segment the electrode contact artifact. ART_C = coil artifact, BOLD = blood oxygen level-dependent, CSF = cerebrospinal fluid, GM = gray matter, GRE-EPI = gradient-recalled echo-echo-planar imaging, ROI_{EPI} = cropped-out artifact region of interest on image from GRE-EPI, ROI_{T1} = cropped-out artifact region of interest on image from T1-weighted MRI, WM = white matter.

Table 4: Summary of Specific Absorption Rates

Sequence	Whole Cohort (<i>n</i> = 56)*	1.5-T MRI (<i>n</i> = 29)*	3-T MRI (<i>n</i> = 27)*	<i>P</i> Value (1.5 T vs 3 T)†
GRE-EPI	0.12 ± 0.10	0.031 ± 0.002 (0.025–0.035)	0.221 ± 0.054 (0.086–0.275)	<.001
T1-weighted 3D SPGR	0.23 ± 0.16	0.078 ± 0.006 (0.063–0.089)	0.397 ± 0.046 (0.257–0.463)	<.001

Note.—Data are for examinations performed with the body transmit-receive coil. Specific absorption rates are given as watts per kilogram. GRE-EPI = gradient-recalled echo–echo-planar imaging, SPGR = spoiled gradient-recalled, 3D = three-dimensional.

* Data are means ± standard deviations. Numbers in parentheses are ranges.

† *P* values are two-sided and were obtained with the two-sample *t* test.

Normalization of the coil and electrode contact artifacts to the standard MNI brain allowed computation of probability maps of signal loss and assessment of brain areas most commonly obscured by the artifacts (Fig 6). These areas included the parietotemporal cortex and deep structures in the immediate vicinity of the electrode contacts. By displaying voxels common to as few as 10 of 100 artifacts, Figure 5 overestimates the area that would be obscured in any single participant.

Visualization of Brain Networks

In participants implanted with neurostimulator, default mode network could be visualized at both 1.5 T and 3 T (Fig E3 [online]).

Discussion

To date, more than 150 000 individuals have been implanted with deep brain stimulation (DBS) devices worldwide. Due to safety concerns, the ability to undergo MRI after DBS implantation is subject to strict regulations. In this study, we sought to provide additional data regarding the MRI safety profile in individuals receiving DBS. We performed structural and functional T1-weighted MRI in 102 study participants with fully internalized and active DBS without short- and long-term adverse effects. Of those 102 participants, 73 underwent 3-T MRI. Our results support the concept that multi-array receive coils—highly desirable for neuroimaging—may be safely used in individuals receiving DBS who undergo 3-T MRI.

Previous studies have used functional MRI to study DBS mechanism of action, however, with important limitations. Our study is an order of magnitude larger than the study by Mueller et al (*n* = 13) (28), which was also limited by a magnetic field strength of 1.5 T. Philipps et al (24) used 3-T MRI in participants receiving DBS; however, their DBS systems were externalized (ie, leads connected to an external pulse generator). This is in contrast with the fully internalized DBS system in our participants, which allows MRI at any time point after surgery.

Different MRI scanners and DBS models were used in our study. The type of neuromodulation systems, MRI hardware, and MRI parameters used are implicated in device heating.

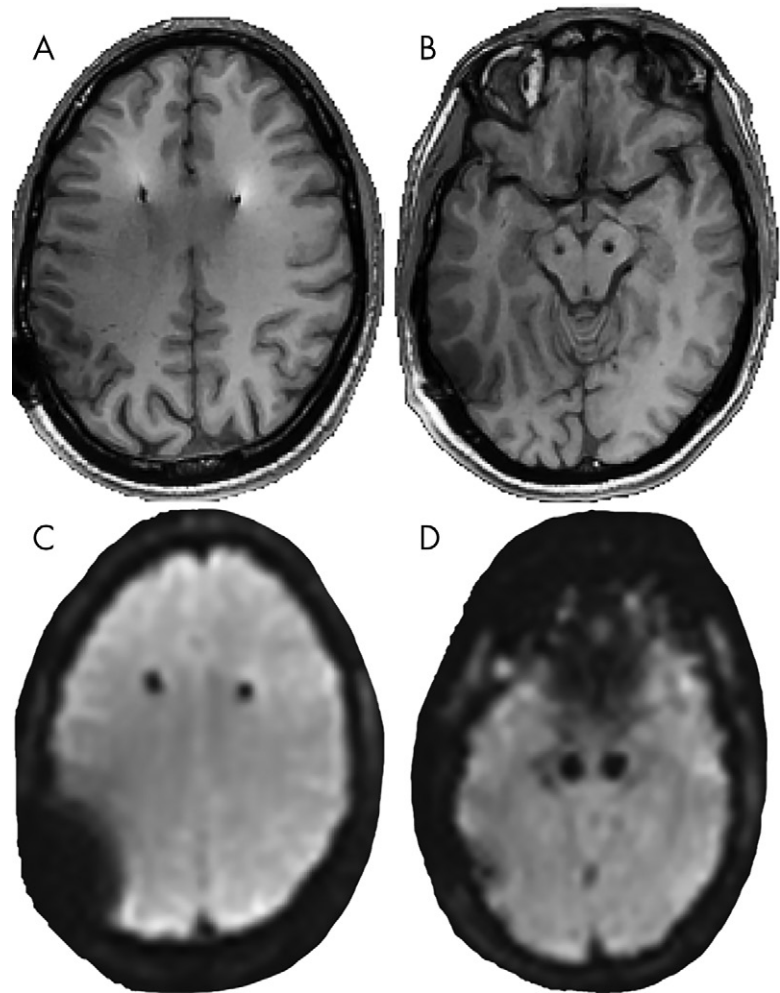


Figure 5: MRI of deep brain stimulation (DBS) device at 3 T. Select images from axial, A, B, three-dimensional spoiled gradient-recalled MRI and, C, D, gradient-recalled echo–echo-planar imaging in participant receiving DBS show the DBS hardware artifact at the level of, A, C, frontoparietal and, B, D, electrode contact artifacts.

Constantly evolving neuromodulation systems may be partly responsible for the inconsistent reported safety data (14,16–19). Importantly, our experience with DBS MRI cannot be generalized to other institutions (specifically their MRI scanners) as previous studies have shown that the temperature rise incited by similar MRI scanners can be variable (21,22). Moreover, the geometry of the neurostimulation device plays a crucial role in

Table 5: DBS Artifact Size at GRE-EPI

Parameter	Whole Cohort (<i>n</i> = 102)*	1.5-T MRI (<i>n</i> = 29)*	3-T MRI (<i>n</i> = 73)*	<i>P</i> Value (1.5 T vs 3 T) [†]
Electrode contact diameter (mm)	9.3 ± 1.6	8.9 ± 1.6 (5.6–11.4)	9.5 ± 1.6 (6.2–12.4)	.1
Proportion of ICV shadowed by single coil artifact (%)	1.9 ± 0.8	1.4 ± 0.7 (0.4–3.4)	2.1 ± 0.7 (0.8–3.6)	<.001
Proportion of gray matter shadowed by single coil artifact (%)	0.98 ± 0.01	0.99 ± 0.01 (0.96–1.00)	0.98 ± 0.01 (0.95–0.99)	<.001

Note.—GRE-EPI = gradient-recalled echo–echo-planar imaging, ICV = intracranial volume.

* Data are means ± standard deviations. Numbers in parentheses are ranges.

[†] *P* values are two-sided and were obtained with the two-sample *t* test.

determining heating (15,18,29), and this geometry may vary across surgeons and institutions. Uncommon DBS configurations such as abdominal IPG would warrant additional safety data. A priori local safety testing and rigorous participant selection for hardware models and geometries previously shown to be safe for MRI is thus crucial.

The extent of the DBS susceptibility artifact depends on a variety of factors, including magnetic field strength and acquisition parameters (30). These artifacts are typically more pronounced at higher field strengths (31). Given that functional MRI spatial resolution is coarse, small differences in artifact sizes between field strengths is unlikely to be meaningful. Our field strength comparison was done with unmatched acquisition parameters. It is well known that echo time plays an important role in artifact size. A larger echo time is associated with larger susceptibility artifacts (30). Echo times were chosen to minimize artifact size while maximizing blood oxygen level–dependent signal (32). Even though our 3-T GRE-EPI pulse sequence used a smaller echo time than its 1.5-T counterpart, the 3-T artifacts remained larger, highlighting the key role of field strength in artifact generation. The improved signal-to-noise ratio at 3 T likely counterbalances the slightly larger artifact size. If desired, techniques to reduce susceptibility artifacts (33) could be used at the higher field strengths.

Because functional MRI sequences (GRE-EPI) are usually associated with more pronounced susceptibility artifact from metallic implants, we sought to characterize areas most commonly obscured by the artifacts on these sequences as these may not be amenable for functional MRI analysis. For the vast majority of participants, coil artifacts remained limited to the superficial lateral parietal and temporal cortex, sparing most of the primary somatosensory cortex—an area previously demonstrated with functional MRI to be integral for therapeutic response to DBS (23). Although not previously thoroughly studied, the location and geometry of the coiled extension wire influence the size and location of the shadowed areas. For improved functional MRI data quality, it is presumably advantageous to have coiled extension placed in between the inion and the mastoid to spare the primary sensorimotor cortex. However, DBS breakage has been reported to be more prevalent when positioned below the mastoid (34). The largest electrode artifact, located distally at the contacts, caused signal loss in neighboring deep

structures. For example, the most common DBS target, the subthalamic nucleus, which is used in the treatment of Parkinson disease, may not be suitable for functional MRI analyses. Using other hubs of the motor circuit, we have shown motor engagement and the utility of functional MRI in programming for individuals receiving DBS (23); however, future functional MRI analysis pipelines for individuals receiving DBS may need to handle missing data resulting from artifact-related voxel effacement.

Our study has some limitations. First, our experience with scanning study participants receiving DBS outside vendor guidelines is not generalizable to other MRI hardware or institutions. To replicate our experience, other institutions would need to also perform local safety testing. However, with careful planning and the appropriate expertise, this can take a few hours without substantial associated cost. Second, the sequences in our study (T1-weighted imaging and GRE-EPI) were inadequate for the detection of acute brain changes such as edema. They were not used as a primary criterion to establish safety. Diagnostic T2-weighted sequences are usually believed to be unsafe for individuals receiving DBS (15). In addition, abnormal signal intensity changes immediately adjacent to the neurostimulator would be masked by the metallic artifact. Third, given that our study participants were scanned with different hardware and software platforms, SAR values may have been estimated in slightly different ways across both institutions. Also, the root-mean-square value of the MRI effective component of the radiofrequency magnetic field (B_1) as an indicator of incident radiofrequency energy would have yielded further safety data. Finally, as newer neuromodulation device models and evolving MRI hardware (eg, 7-T MRI) are developed, additional safety experiments will need to be done.

In conclusion, our experience with deep brain stimulation (DBS) MRI demonstrates that (a) MRI of individuals receiving DBS outside prescribed vendor guidelines may be done safely and (b) functional MRI data are amenable for analysis despite the susceptibility artifacts. Phantom experiments allow a better understanding of the relationships between these implants and their safe MRI use. Alternative pulse sequences and higher field strengths, which may be outside current vendor guidelines, will likely be incorporated into neuroimaging protocols. Individuals receiving DBS will benefit from additional MRI safety knowledge as it offers the potential to expand their MRI possibilities and provide further research tools.

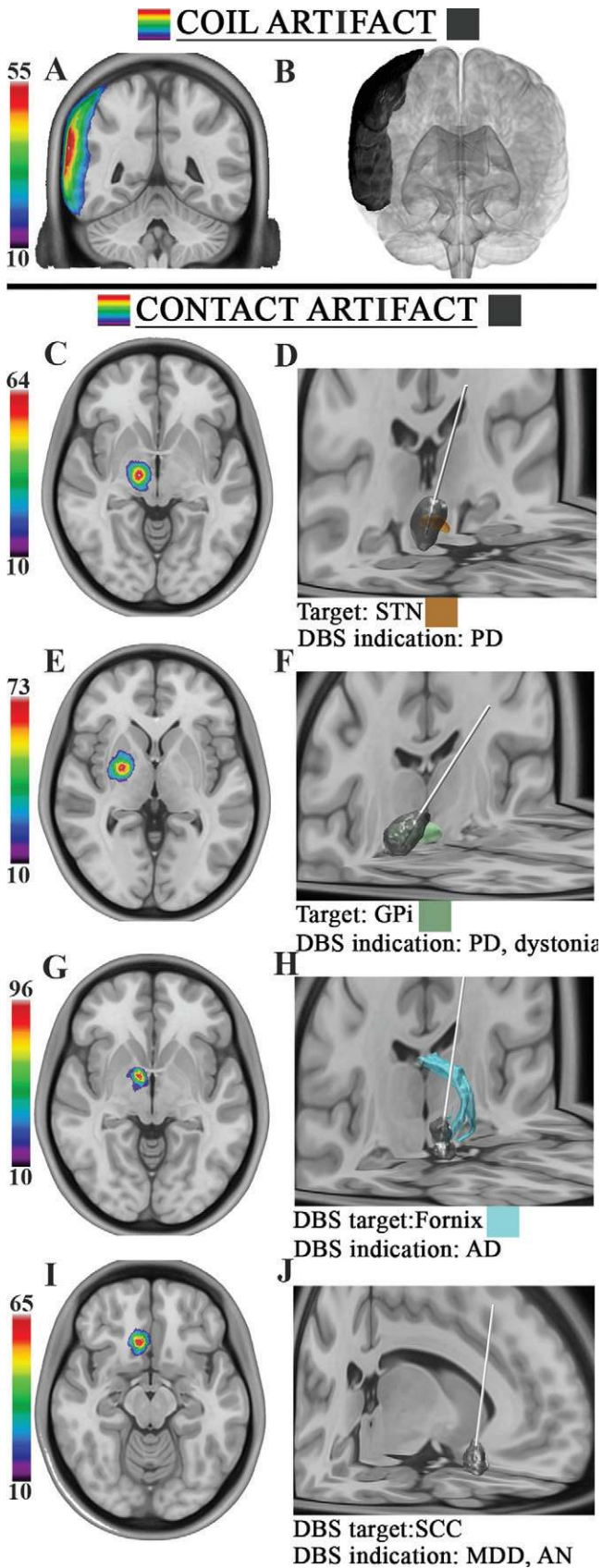


Figure 6: Deep brain stimulation (DBS) artifact distributions. DBS hardware artifact probability maps for, *A, B*, coil artifact and, *C–J*, DBS electrode contacts included in study cohort. For group analysis, individual participant's coil and electrode contact artifacts were transformed (ie, normalized) to a standard brain (MNI brain). Left-sided artifacts were flipped on the right side. Artifact frequency maps were then obtained by summing the artifacts and then dividing by the size of each group (color bar unit = percentage). *A, C, E, G, I*, Two-dimensional frequency maps are shown on axial T1-weighted images from MRI of brain. Frequency maps were thresholded at 10% (ie, these voxels were only shadowed in 10% of participants) for visualization. Right and left on the images follow radiologic conventions. *B, D, F, H, J*, Three-dimensional reconstructions of frequency maps are shown in T1-weighted MNI brain image with relevant DBS target. Three-dimensional visualization of DBS targets was done with the Lead-DBS toolbox (www.lead-dbs.org). Note that the anterior thalamic nucleus contact artifact map was not included because it applied to only one participant. AD = Alzheimer disease, AN = anorexia nervosa, GPi = globus pallidus interna, MDD = major depressive disorder, PD = Parkinson disease, SCC = subcallosal cingulate cortex, STN = subthalamic nucleus.

Acknowledgments: We thank Michael Gilgoly, RN, for performing clinical examinations before and after MRI. We also acknowledge the contributions of the late Eugen Hlasny, MRT(MR), MRI technologist at the University Health Network.

Author contributions: Guarantors of integrity of entire study, A.B., R.M.G., V.P., S.P., D.G., A.M.L.; study concepts/study design or data acquisition or data analysis/interpretation, all authors; manuscript drafting or manuscript revision for important intellectual content, all authors; approval of final version of submitted manuscript, all authors; agree to ensure any questions related to the work are appropriately resolved, all authors; literature research, A.B., I.H., R.M.G., B.L., S.P., A.C., S.K.K., W.K., A.M.L.; clinical studies, A.B., I.H., R.M.G., M.D., B.L., V.P., S.P., M.R., D.S., E.F., S.K.K., W.K., J.P., A.M.L.; experimental studies, A.B., T.R., I.H., G.J.B.E., R.G., J.G., M.D., B.L., V.P., S.P., M.R., D.S., E.F., M.H., W.K., J.P.; statistical analysis, A.B., G.J.B.E., R.M.G., J.G., S.P., C.T.C., A.M.L.; and manuscript editing, A.B., T.R., I.H., G.J.B.E., R.M.G., J.G., M.D., B.L., V.P., S.P., M.R., A.C., D.G., R.M., D.S., E.F., M.H., S.K.K., A.F., W.K., J.P., A.M.L.

Disclosures of Conflicts of Interest: **A.B.** Activities related to the present article: disclosed no relevant relationships. Activities not related to the present article: institution receives money from GE Global Research. Other relationships: disclosed no relevant relationships. **T.R.** disclosed no relevant relationships. **I.H.** disclosed no relevant relationships. **G.J.B.E.** disclosed no relevant relationships. **R.M.G.** disclosed no relevant relationships. **J.G.** disclosed no relevant relationships. **M.D.** disclosed no relevant relationships. **B.L.** disclosed no relevant relationships. **V.P.** disclosed no relevant relationships. **S.P.** disclosed no relevant relationships. **M.R.** disclosed no relevant relationships. **A.L.** Activities related to the present article: institution received a grant from GE Healthcare; received a consulting fee or honorarium from Medtronic, St. Jude, and Boston Scientific. Activities not related to the present article: is a paid consultant for Medtronic, St. Jude, and Boston Scientific. Other relationships: disclosed no relevant relationships. **D.G.** disclosed no relevant relationships. **C.T.C.** disclosed no relevant relationships. **R.M.** disclosed no relevant relationships. **D.S.** disclosed no relevant relationships. **E.F.** disclosed no relevant relationships. **M.H.** disclosed no relevant relationships. **S.K.K.** Activities related to the present article: disclosed no relevant relationships. Activities not related to the present article: is a paid consultant for Medtronic; received grants/grants pending from CIHR; received payment for lectures including service on speakers bureaus from Medtronic. Other relationships: disclosed no relevant relationships. **A.F.** disclosed no relevant relationships. **W.K.** disclosed no relevant relationships. **J.P.** Activities related to the present article: received a grant from GE Global Research. Activities not related to the present article: is a paid consultant for Boston Scientific, Nevro, Jazz Pharmaceuticals, and Abbott; received payment for expert testimony from Aim Medical Robotics and Karuna; has grants/grants pending from Medtronic, Boston Scientific, Abbott, Jazz Pharmaceuticals, and GE Global Research; has stock/stock options in Aim Medical and Karuna. Other relationships: disclosed no relevant relationships. **A.M.L.** Activities related to the present article: institution received a grant from GE Healthcare; received consulting fee or honorarium from Medtronic, St. Jude, and Boston Scientific. Activities not related to the present article: is a paid consultant for Medtronic, St. Jude, and Boston Scientific. Other relationships: disclosed no relevant relationships.

References

- Lozano AM, Lipsman N. Probing and regulating dysfunctional circuits using deep brain stimulation. *Neuron* 2013;77(3):406–424.
- Kringelbach ML, Jenkinson N, Owen SL, Aziz TZ. Translational principles of deep brain stimulation. *Nat Rev Neurosci* 2007;8(8):623–635.
- Lozano AM, Lipsman N, Bergman H, et al. Deep brain stimulation: current challenges and future directions. *Nat Rev Neurol* 2019;15(3):148–160.
- Wichmann T, Delong MR. Deep brain stimulation for neurologic and neuropsychiatric disorders. *Neuron* 2006;52(1):197–204.
- Hariz M. My 25 Stimulating Years with DBS in Parkinson's Disease. *J Parkinsons Dis* 2017;7(s1):S33–S41.
- Boston Scientific. ImageReady MRI Guidelines for Boston Scientific Deep Brain Stimulation Systems. Boston, Mass: Boston Scientific, 2017; 613.
- Medtronic. MRI guidelines for Medtronic deep brain stimulation systems. Dublin, Ireland: Medtronic, 2015; 44.
- St. Jude Medical. MRI procedure information for St. Jude Medical MR conditional deep brain stimulation systems. Saint Paul, Minn: St. Jude Medical, 2018; 23.
- Zrinzo L, Yoshida F, Hariz MI, et al. Clinical safety of brain magnetic resonance imaging with implanted deep brain stimulation hardware: large case series and review of the literature. *World Neurosurg* 2011;76(1-2):164–172; discussion 69–73.
- Henderson JM, Tkach J, Phillips M, Baker K, Shellock FG, Rezaei AR. Permanent neurological deficit related to magnetic resonance imaging in a patient with implanted deep brain stimulation electrodes for Parkinson's disease: case report. *Neurosurgery* 2005;57(5):E1063; discussion E1063.
- Spiegel J, Fuss G, Backens M, et al. Transient dystonia following magnetic resonance imaging in a patient with deep brain stimulation electrodes for the treatment of Parkinson disease. Case report. *J Neurosurg* 2003;99(4):772–774.
- Cheng CH, Huang HM, Lin HL, Chiou SM. 1.5T versus 3T MRI for targeting subthalamic nucleus for deep brain stimulation. *Br J Neurosurg* 2014;28(4):467–470.
- Verhagen R, Schuurman PR, van den Munckhof P, Contarino MF, de Bie RM, Bour LJ. Comparative study of microelectrode recording-based STN location and MRI-based STN location in low to ultra-high field (7.0 T) T2-weighted MRI images. *J Neural Eng* 2016;13(6):066009.
- Bhidayasiri R, Bronstein JM, Sinha S, et al. Bilateral neurostimulation systems used for deep brain stimulation: in vitro study of MRI-related heating at 1.5 T and implications for clinical imaging of the brain. *Magn Reson Imaging* 2005;23(4):549–555.
- Boutet A, Hancu I, Saha U, et al. 3-Tesla MRI of deep brain stimulation patients: safety assessment of coils and pulse sequences. *J Neurosurg* doi: 10.3171/2018.11.JNS181338. Published online February 22, 2019. <https://doi.org/10.3171/2018.11.JNS181338>.
- Carmichael DW, Pinto S, Limousin-Dowsey P, et al. Functional MRI with active, fully implanted, deep brain stimulation systems: safety and experimental confounds. *Neuroimage* 2007;37(2):508–517.
- Kahan J, Papadaki A, White M, et al. The Safety of Using Body-Transmit MRI in Patients with Implanted Deep Brain Stimulation Devices. *PLoS One* 2015;10(6):e0129077.
- Rezaei AR, Finelli D, Nyenhuis JA, et al. Neurostimulation systems for deep brain stimulation: in vitro evaluation of magnetic resonance imaging-related heating at 1.5 Tesla. *J Magn Reson Imaging* 2002;15(3):241–250.
- Sammartino F, Krishna V, Sankar T, et al. 3-Tesla MRI in patients with fully implanted deep brain stimulation devices: a preliminary study in 10 patients. *J Neurosurg* 2017;127(4):892–898.
- Rezaei AR, Phillips M, Baker KB, et al. Neurostimulation system used for deep brain stimulation (DBS): MR safety issues and implications of failing to follow safety recommendations. *Invest Radiol* 2004;39(5):300–303.
- Baker KB, Tkach JA, Nyenhuis JA, et al. Evaluation of specific absorption rate as a dosimeter of MRI-related implant heating. *J Magn Reson Imaging* 2004;20(2):315–320.
- Baker KB, Tkach JA, Phillips MD, Rezaei AR. Variability in RF-induced heating of a deep brain stimulation implant across MR systems. *J Magn Reson Imaging* 2006;24(6):1236–1242.
- Hancu I, Boutet A, Fiveland E, et al. On the (Non-)equivalency of monopolar and bipolar settings for deep brain stimulation fMRI studies of Parkinson's disease patients. *J Magn Reson Imaging* 2019;49(6):1736–1749.
- Phillips MD, Baker KB, Lowe MJ, et al. Parkinson disease: pattern of functional MR imaging activation during deep brain stimulation of subthalamic nucleus—initial experience. *Radiology* 2006;239(1):209–216.
- Hiss S, Hesselmann V, Hunsche S, et al. Intraoperative functional magnetic resonance imaging for monitoring the effect of deep brain stimulation in patients with obsessive-compulsive disorder. *Stereotact Funct Neurosurg* 2015;93(1):30–37.
- Lempka SF, Johnson MD, Miodinovic S, Vitek JL, McIntyre CC. Current-controlled deep brain stimulation reduces in vivo voltage fluctuations observed during voltage-controlled stimulation. *Clin Neurophysiol* 2010;121(12):2128–2133.
- Satzer D, Lanctin D, Eberly LE, Abosch A. Variation in deep brain stimulation electrode impedance over years following electrode implantation. *Stereotact Funct Neurosurg* 2014;92(2):94–102.
- Mueller K, Jech R, Růžicka F, et al. Brain connectivity changes when comparing effects of subthalamic deep brain stimulation with levodopa treatment in Parkinson's disease. *Neuroimage Clin* 2018;19:1025–1035.
- Baker KB, Tkach J, Hall JD, Nyenhuis JA, Shellock FG, Rezaei AR. Reduction of magnetic resonance imaging-related heating in deep brain stimulation leads using a lead management device. *Neurosurgery* 2005;57(4 Suppl):392–397; discussion 392–397.
- Port JD, Pomper MG. Quantification and minimization of magnetic susceptibility artifacts on GRE images. *J Comput Assist Tomogr* 2000;24(6):958–964.
- Farahani K, Sinha U, Sinha S, Chiu LC, Lufkin RB. Effect of field strength on susceptibility artifacts in magnetic resonance imaging. *Comput Med Imaging Graph* 1990;14(6):409–413.
- Gati JS, Menon RS, Ugurbil K, Rutt BK. Experimental determination of the BOLD field strength dependence in vessels and tissue. *Magn Reson Med* 1997;38(2):296–302.
- In MH, Cho S, Shu Y, et al. Correction of metal-induced susceptibility artifacts for functional MRI during deep brain stimulation. *Neuroimage* 2017;158:26–36.
- Blomstedt P, Hariz MI. Hardware-related complications of deep brain stimulation: a ten year experience. *Acta Neurochir (Wien)* 2005;147(10):1061–1064; discussion 1064.